Functional and structural parameters of a paved road section constructed with mixed recycled aggregates from non-selected construction and demolition waste with excavation soil

Javier Tavira[a, *], José Ramón Jiménez[b, *], Jesús Ayuso[b], María José Sierra[c], Enrique Fernández Ledesma[d]

[a] JTD Civil Eng., Carretera de Carmona 40 D 1º D 41008 Sevilla, Spain.

[b] Área de Ingeniería de la Construcción, Universidad de Córdoba. Ctra. N-IV, Km 396, 14014 Córdoba, Spain.

[c] Agencia de la Obra Pública. Consejería de Fomento y Vivienda. Junta de Andalucía. Av. Diego Martínez Barrio, 10, 41013 Sevilla, Spain.

[d] Área de Mecánica de Medios Continuos y Teoría de Estructuras, Universidad de Córdoba. Ctra. N-IV, Km 396, 14014 Córdoba, Spain.

*Corresponding authors. Both authors equally contributed to the paper. Address: Construction Engineering Area. University of Córdoba, Ed. Leonardo Da Vinci, Campus de Rabanales, Ctra. N-IV, km-396, CP 14014. Córdoba, Spain. Tel.: +34 667524702; fax: +34 957218550.

E-mail address: jrjimenez@uco.es (JR Jiménez), jtavira@ciccp.es (J. Tavira)

Abstract

This paper evaluates the lab and in situ mechanical properties of non-selected mixed recycled aggregates from construction and demolition waste (CDW) used as base and subbase unbound materials. Excavation materials are mixed with CDW to produce recycled mixed aggregates with soil, as well as a finer material referred to as mixed recycled soil. The research was divided into two different stages: a laboratory study characterizing the properties of recycling aggregates and a road test track evaluating the long-term performance of these materials under real traffic and weather conditions. During construction, several density, plate load, and falling weight deflectometer tests were performed to determine the bearing capacity of all layers. A laser profiler was also used to obtained the international roughness index. After the road was opened to traffic, a follow up of deflections and surface roughness was performed during the following seven years.

Two different moduli calculation methods were used: back calculation and forward calculation. Both methods shown acceptable values for these recycled materials. Low quality recycled mixed aggregates can be used as substitutes for natural aggregates as unbound layers. The mechanical performance and surface roughness values obtained from the experimental road shown an acceptable behaviour.

Keywords:

Construction and demolition waste, mixed recycled aggregates, backcalculation, forward calculation, International Roughness Index, experimental road.

Acronyms:

CDW - construction and demolition waste; RMAS - Recycled mixed aggregates with excavation soil; MRS - Mixed Recycled soil; FWD - falling weight deflectometer; IRI - International Roughness Index; NA - natural aggregates; RA - recycled aggregates; RCA - recycled concrete aggregates; CBR - California Bearing Ratio; ER - experimental road; NDT - nondestructive testing; CS - crushed stone; SS - selected soil; SG - subgrade; GPR - ground penetrating radar; PG3 - Spanish general technical specification for road construction.

1. Introduction

The construction sector contributes significantly to greenhouse gas emissions because of the use of heavy machinery and because of cement production; these emissions contribute greatly to climate change (UE Directive 2010/31/EC). Additionally, construction activities consume a large quantity of non-renewable natural resources, such as aggregates, which are scarce in many countries. To reduce these negative effects and contribute to the sustainability of the sector, it is necessary to promote the use of recycled aggregates (RA) from construction and demolition waste (CDW). This will provide a second life cycle to raw materials [1].

In 2009 approximately 530 million tonnes of CDW were produced in the European Union [2]. Spain produced 26 million tonnes in 2012 [3]. If the excavation soils from construction activities were included, the total waste would be 1350 to 2900 million tonnes [4]. These data show the importance of CDW and excavated soils to waste generation. According to the European Commission, 25−30% of total generated solid waste comes from construction. The recycling rate in Spain reached 30% in 2011 [5], which is below the EU-27 average (47%) [5] and it much lower than that in other European countries such as Germany (86%) or Denmark (94%) [2]. The waste framework directive of the European Parliament on waste stipulated that by 2020, a minimum recycling level must be achieved of 70% of non-hazardous CDW [6].

The possibility of using RA from CDW in road construction has been studied by many researchers. Vegas et al. [7], Garcia [8], Poon et al. [9] and Jiménez et al. [10–12] assessed the feasibility of using RA as a granular material in the structural layer of pavement. Vegas et al.[7] and Jiménez et al.[10–12] concluded that the most critical properties are sulphur content because it can generate dimensional unstability of the layer and fragmentation resistance which is deeply related with durability. Jiménez et al. [10–12] compared the behaviour of RA from CDW with that of natural aggregates (NA) on unpaved rural roads. They concluded that RA can be used as an alternative to NA on unpaved roads. Few studies on the mechanical capacity of RA have been made on experimental road sections [13].

In a laboratory study, Del Rey et al. [14] found that cement-treated RA in a size range of 0−8 mm can be used as a subbase layer for light-traffic roads. Agrela et al. [15] performed tests on a road section constructed with recycled mixed aggregates (RMA) in Malaga (Spain), and concluded that RMA treated with 3% cement can be used in the subbase layers of roads. Perez et al. [16] used recycled concrete aggregates (RCA) and natural aggregates (NA) treated with cement as sub-base layers in two road test sections. Deflections showed that RCA had a higher bearing capacity although a higher percentage of water was needed.

Cardoso et al. [17] reviewed the use of RA in geotechnical applications, mainly the use of CDW in pavement layers. Several studies were performed on pavements made with NA, RCA, and RMA; these produced several conclusions regarding the bearing capacity, durability, and workability of RA relative to NA. The international roughness index (IRI) and deflections were similar in both materials, with RA performing better. RMA and RCA have a higher optimum water content than NA. The Californian bearing ratio (CBR) of RMA was lower than that of NA, but it could be increased by adding RCA.

There has been some international experience with RMA and RA used in low volume traffic roads. In China [18], RA obtained from concrete and bricks waste was used in bases and sub-bases. Cement was added, and deflection tests were made comparing RMA and RCA stabilized with cement and limestone. The main conclusion was that RA treated with cement are feasible for road pavement construction.

Park [19] used two road sections constructed from variable-quality RCA and compared them with those constructed from NA, obtaining similar deflections. Lancieri et al [20] performed a long-term test using RMA as an unbound layer in two paved sections, obtaining elastic moduli for these recycled unbound layers over a period of eight years. These materials showed an increase in bearing capacity due to self-cementing and further traffic compaction.

The elastic modulus is a basic input needed to calculate stress-strain values for pavement. Mechanical durability is deeply connected with this parameter.

This paper has two main purposes. The first one is to study the short and long-term performance of low quality recycled materials obtained from non-selected CDW mixed with excavated soils. The second one is to calculate the elastic moduli of these materials in an experimental road (ER) using nondestructive testing (NDT) such a FWD. The elastic modulus of each layer can be determined using the deflection basin [21]. This way, the mechanical properties of these materials can be obtained, assuring the bearing capacity of the road.

Because of the high amount of excavated soil obtained from construction sites [4,13], it is quite important to find new applications for these wastes. To the best of the authors' knowledge, there are no previous studies investigating RA mixed with excavated soils and used as unbound layers in roads. RMA with soil (RMAS) could also be a good material for reducing plasticity of the excavated wastes, because RA has no expansive properties [13]. To test the viability of RA used in unbound layers in road pavements, it is critical to reproduce real scale models. It is fundamental to perform middle- and long-term evaluations to verify the consistency of RA in these uses. Because of the duration of the present study, this target has been achieved. It also fills a gap in the availability of long-term performance studies on recycled materials used in roads open to traffic.

2. Materials and methods

2.1 Description of test sections

The experimental road (ER) was built on the service road of a four-lane freeway in Seville (south of Spain). The ER consists of three sections, each one 150 m long (total length of 450 m). Fig.1 shows a description of the three sections and the thicknesses of the structural layers. The surface course for all sections consists of 5 cm of asphalt concrete. The base course of the first two sections is a crushed limestone (CS-1) used as a reference and a recycled mixed aggregate from non-selected CDW with excavation soil (RMAS-1). In the third section, granular base course materials would be classified as a A1a, according to AASHTO [22]. The subbase course was built with two different materials, a natural selected soil, which would be classified as A3 according to AASHTO [22] (SS-1), and a mixed recycled soil (MRS-1) from preliminary screening in sections I.II and I.III, which would be classified as A4 [22]. Construction of the ER lasted from February to June of 2009.

The two basic characteristics of this road are as follows:

•Traffic intensity is homogeneous for all sections investigated. Traffic counting was performed from the September 5th 2016 (Monday) to September 11th 2016 (Sunday). The mean value for heavy vehicles was 30 per day, from a total of 659. According to Spanish standards [23] this road would be classified as a T41 (25-49 heavy vehicles/day).

• The subgrade has the same composition in the three sections. It is a red silty clay, classified as A6 in accordance with AASHTO [22] (SG-1).

2.2 CDW treatment process

Two recycled materials (MRS-1 and RMAS-1) were collected from a recycling plant located 5 km north of the ER (Sevilla, Spain). Fig.2 shows a schematic of the process followed to obtain both recycled materials. MRS-1 was obtained from the preliminary screening process (20 mm sieve) of a non-selected CDW mixed with excavation soils. The excavated soil came from construction sites around the recycling plant, basically this material came from foundations and ditches excavations. When excavation soils are not reused in-situ, they must be managed by an authorized recycling plant. In this case, the excavation soils were mixed with the non-selected CDW in the recycling plant.

To obtain RMAS-1, the material larger than 20 mm was crushed in an impact crusher and screened with a 40 mm sieve. A magnetic conveyor belt was used to remove metallic elements.

2.3 Material characterisation

The samples used to characterise the materials were collected prior to compaction during the construction of the ER, according to UNE-EN 932-1:1997 [24]. Samples were homogenised and reduced in a laboratory using a quartering method, according to UNE-EN 932-2:1999 [25].

Table 1 presents the compositions of MRS-1 and RMAS-1, determined according to UNE-EN 933-11:2009 [26]. MRS-1 has a high percentage of natural soil from excavation; no other previous research has been found of a RMA with these characteristics. According to Agrela et al. [27], Jiménez [13], and Cardoso et al. [17], both MRS-1 and RMAS-1 due its elevated content of natural soil would be unclassified RA.

Both of the natural materials (SS-1 and CS-1) came from limestone quarries. All of the parameters fulfilled the requirements of articles 330 (SS-1) and 510 (CS-1) of the Spanish general technical specification for road construction (PG3) [28]. Table 2 shows the primary mechanical, physical, and chemical properties of these materials. The densities and CBRs of NA are higher than those of MRS-1 and RMAS. The CBR value for recycled materials falls between previous values obtained for RMA 69−90 % [13,14]. The optimum moisture is higher for recycled materials than natural materials.

Based on their mechanical properties, all granular materials used in the ER (MRS-1, SS-1, RMAS-1 and CS-1) meet the limits established by PG3 for use as road materials, except for the Los Angeles test of RMA-1, which was not under the 35 % limit (PG3). According to previous literature, most values for RMA fall between 35 and 43% [13,20], local specifications for RMA raise this value to 50% [29].

With respect to chemical properties, PG3 imposes a 0.2 % limit on the content of organic matter and soluble salts for a granular sub-base. This limit decreases to 0.07 % in granular bases. Previous studies [10,12,13] showed that soluble salt content below 3.74% does not create stability problems. Organic matter is not a limiting property in road applications, and has a typical range of 0.42-1.00 % according to Jimenez [13].

The sand equivalent in RMAS-1 does not meet the PG3 minimum value of 35%. Previous studies of recycled materials used as unbound layers did meet these limits [10,12].

Particle size distribution was studied in accordance with standard UNE-EN-933-1:2006 [30]. As shown in Fig. 3, both materials have less than 10% of fine fraction (< 0.063 mm), and the coefficients of uniformity and gradation are very similar in both materials.

2.4 Description of external factors

Climate has a great influence on the behaviour of pavement layers. Precipitation and temperature values were collected from a nearby weather station located in Los Molares (Seville) with UTM coordinates (262696, 4117760).

Fig. 4 shows the average monthly maximum and minimum temperatures. From 2009 to 2016, there were no extreme temperatures. Fig. 5 shows that the highest observed rainfall (912 mm) occurred in 2010. The driest year was 2012, with only 405 mm. Total rainfall was 460 mm in 2011 and 555 mm in 2009. Major rains occurred from November to March during the period of lowest temperatures, meaning that monthly rain during this period was 49 mm.

2.5 Tests in site

2.5.1 Control of compaction

Moisture and dry density was measured using a Troxler apparatus during the construction of the road in May 2009. Five measurements were measured on each section of the subbase and base course. The tests were performed according to ASTM-D-6938:15 [31].

2.5.2 Plate load tests

Six static plate load tests were performed, one on each of the three sections of the sub-base and base course, in accordance with Spanish standard UNE 103808:2006 [32]. A 200 kN load device and 300 mm diameter steel plate were used. The strain moduli Ev1 and Ev2 (first and second load cycle) were measured. Tests were performed during construction of the road in May 2009.

2.5.3 Falling weight deflectometer (FWD)

Pavement deflection is commonly accepted as a state indicator of pavement structural conditions [33]. This test consists of the bearing capacity determination of each layer, starting at the subbase. A Dynatest Heavy Weight Deflectometer 8081 equipped with seven geophones was used. The geophones were located at 0-300-450-600-900-1200-1500 mm. This equipment has been used in previous studies (see Jimenez et al [10,12]).

A 450 mm diameter plate was used for the granular layers (bases and subbases), and a 300 mm diameter was used on surfaced courses. Loads of 39.24 kN were applied with a pressure of 246.47 kPa on subbases, loads of 68.67 kN were applied with a pressure of 431.33 kPa on bases, and loads of 49.05 kN were applied with a pressure of 693.21 kPa on surface courses, the standard that regulates these loads and configurations is the "Technical Specifications for High-Performance Dynamic Monitoring Tests" [34] from the Civil Works Agency of Regional Government of Andalusia (Spain).

Deflections were obtained every 20 m along the three sections, in accordance with ASTM D4694 (2003). According to Spanish standard, temperature did not influence the measurement of the deflection located under the plate at a distance of 0 mm. This occurred because the asphalt concrete was less than 10 cm thick [33].

Fig. 6 shows the theoretical deflection calculated with multilayer software BISAR [35]. This software applies the theories of Burmister [36] and Acum and Fox [37], and is implemented with a solution for determining strain and stress by Shiffmann [38]. The theoretical deflection was obtained for each layer and section according to the elastic moduli and Poisson ratios. Poisson ratio values were adopted of 0.35 (for granular layers and roadbed soil), and 0.33 (for the bituminous layer) [39,40]. Roadbed moduli were determined from CBR tests performed along the section using the correlation described in the pavement instruction of Andalusia (Spain) [39].

2.5.4 Laser profiler (LP)

Road roughness strongly influences operation costs, and is generally related to the regularity of pavement surfaces. Globally, the accepted parameter for establishing the smoothness of roads is the IRI [41], which was calculated according to ASTM E867-06:2012 [42]. There are correlations with the present serviceability index (PSI), another important index [43]. A new road has a PSI value of 4.5, which is equivalent to a 0.285 m/km IRI, while a road at the end of its life has a PSI value of 2, which is equivalent to a 4.45 m/km IRI. Longitudinal profile data was collected in 2009 and 2016 to study IRI evolution over time. The IRI was measured using a RSP MARK-IV device, which was previously used in the studies of Jimenez et al [10,12]. Eight passes were conducted for each IRI mean value. Data were analysed using a one-way analysis of variance (ANOVA).

2.6 Elastic modulus calculation

2.6.1 Back calculation using RMS

Back calculation is the main method used to calculate moduli [44]. This method consists of comparing the theoretical deflections in the road with the actual data obtained from a FWD. It is an iterative process in which the error tends to be minimized at each step [45]. The moduli for bases and subbases were obtained from Evercalc [45]. In essence, this software calculates a deflection basin until it matches the measured deflections. The required inputs are layer thickness, Poisson ratio, and the seed moduli for each layer. Tolerable error is calculated using the root mean square (1).

$$\boldsymbol{RMS}\ (\%) = \left[\sqrt{\frac{1}{n_d}}\sum_{i=1}^{n}\left[\frac{d_{ci}-d_{mi}}{d_{mi}}\right]^2\right]\cdot \mathbf{100} \qquad \textbf{(1)}$$

Where:

RMS = root mean square error,

d_{ci} = calculated pavement surface deflection at sensor i,

d_{mi} = measured pavement surface defection at sensor i,

n_d = number of deflection sensors used in the back calculation process.

Seed moduli are the initial moduli used in the computer program to calculate surface deflections. Evercalc uses WESLEA [46] as the layered elastic solution to compute theoretical deflections, and uses a modified Augmented Gauss-Newton algorithm for optimization. The process is terminated when the error is tolerable or when the maximum number of iterations is reached.

2.6.2 Forward calculation

Another way to determine the mechanical properties of pavement layers is through the use of forward calculation [47]. This is an empirical approach for the calculation of the flexible and rigid pavement layer moduli developed by Stubstad et al. [47]. It involves estimating the modulus of the pavement using the Hogg model [48], whose implementation is described by Wiseman [49]. Three cases are considered. Cases I and II are for subgrades with Poisson ratios of 0.4 and 0.5, respectively. Case III allows any value to be used as the Poisson ratio. The adimensional constants used for the three approaches in the Hogg model are presented in Table 3. The most fittable version for the characteristics of the ER is case number III, which uses a Poisson ratio of 0.35 for roadbed soil.

The following equations are used:

$$\boldsymbol{E_0 = I \cdot \frac{(1+v_0)*(3-4*v_0)}{2*(1-v_0)} \cdot \left[\frac{S_0}{S}\right] \cdot \left[\frac{p}{D_0*l}\right]} \tag{2}$$

Where: E_0 = subgrade modulus, v_0 = Poisson ratio, S_0 = theoretical point load stiffness, S = pavement stiffness, p = applied load, D_0 = deflection from centre plate, l = characteristic length, I = Influence factor, m = characteristic length coefficient, $\overline{m}$ = stiffness ratio coefficient.

$$\boldsymbol{r_{50} = r \cdot \frac{(1/\alpha)^{1/\beta} - B}{\left[\frac{1}{\alpha} * \left[\frac{D_0}{D_r} - 1\right]\right]^{1/\beta} - B}} \tag{3}$$

Where: D_r = deflection at offset distance r, r = distance from centre of load plate, B = curve fitting coefficient, b = curve fitting coefficient, a = curve fitting coefficient,

$$\boldsymbol{l = y_0 \cdot \frac{r_{50}}{2} + [(y_0 \cdot r_{50})^2 - 4 \cdot m \cdot \alpha \cdot r_{50}]^{0.5}} \quad \textbf{(4)}$$

Where: y_0 = characteristic length coefficient, r_{50} = offset distance where D_r/D_0=0.5.

$$\boldsymbol{\left[\frac{S}{S_0}\right] = 1 - \bar{m} \cdot \left[\frac{\alpha}{l} - 0.2\right]} \quad \textbf{(5)}$$

If a/I < 0.2 then $\left[\frac{S}{S_0}\right] = 1.0$

The second step is to use the subgrade modulus to determine the moduli for subbases and bases using equation (6) [50].

$$\boldsymbol{E_i = 0.2 \cdot {h_i}^{0.45} \cdot E_{i+1}} \quad \textbf{(6)}$$

Where: E_i = modulus of the upper layer, E_{i+1} = modulus of the lower layer, h_i = thickness of the upper layer.

Dynamic moduli from these granular base and subbase deflections were calculated by the following equation, proposed by Brown [51]:

$$\boldsymbol{E_0 = \frac{2\sigma_0 a(1-\mu_0^2)}{d_0}} \quad \textbf{(7)}$$

Where: E_0 = equivalent modulus of the entire pavement system beneath the load plate, a = radius of the FWD plate, σ_0 = Pressure of the FWD impact load under the load plate d_0 = deflection at 0 mm at the centre of the FWD plate.

3 Results and discussion

3.1 Quality control of compaction

Figs. 7 and 8 show the dry density and moisture content of the subbase and base layers during construction. The compaction values obtained for the base and subbase course layer were above 98% and 95%, respectively, in the modified proctor. This means that the values meet the limits in PG3 articles 330 and 510 [28]. However, the compaction water content was lower than the optimum moisture obtained in the laboratory, possibly because of the lack of experience using RA by the construction companies and supervising engineers.

According to Fig. 7, results for the subbases show that the densities for MRS-1 (sections I.II and I.III) are lower than those for conventional soil SS-1 (section I.I). In base layers, densities are also lower for recycled materials (RMAS-1) than for crushed quarry (CS-1), as shown in Fig. 8. These results are in line with previous studies carried out by Jiménez et al. [9–12] and Del Rey et al. [14].

Fig. 7 shows that moisture content is similar for the three section materials. In MRS-1, there is an important gap between the optimum moisture content and the content obtained on site. Fig. 8 shows similar results for the base layers. Materials were placed in work with a moisture content below the optimum value obtained in laboratory tests. This is attributable to the lower dry density and higher water absorption capacity of recycled aggregates relative to NA. Jiménez [13] proposed that in recycled mixed aggregates the water absorption values range from 11 to 15%, while in NA this value range from 0.5 to 1.8%.

This work has shown that the quality control of compaction and moisture of mixed recycled aggregates placed on site has to be higher than for natural aggregates, since recycled aggregates require a greater amount of compaction water and the construction companies have no experience in the use of mixed recycled aggregates.

3.2 Loading test plate results

The deformation moduli in subbases are similar for recycled materials, while the selected soil of section I.I is higher. As shown in Fig. 9, the ratio between both cycles is higher than 2 in MRS-1 and lower than 2 in quarry materials (SS-1), which can be justified by the lower compaction percentage of MRS-1 with respect to SS-1 (Fig. 7).

Deformation moduli on granular bases are similar in sections I.I and I.II. The modulus for section I.III is lower, as shown in Fig. 10. The ratio between Ev1 and Ev2 seems to be lower than 2 for CS-1 and RMAS-1, which means that high compaction has been obtained during the placement on site (Fig. 8).

The plate load test in Fig. 9 and Fig. 10 shows values over 200 MPa for the E_{v2} in bases and subbases. The ratio between E_{v2} and E_{v1} is below 2.2; these values comply with Spanish standards [28] limits for foundation failure by vertical strain.

Despite the good bearing capacity of the recycled materials used in this study, the moduli obtained in this work are lower than those obtained by Jiménez et al. [10] on an experimental unpaved rural road. These authors tested a selected mixed recycled aggregate, a recycled concrete aggregates and a crushed limestone as reference. The layers built using recycled aggregates showed a high bearing capacity, the Ev_2 values oscillated between 270 and 405 MPa for mixed recycled aggregates and 321 and 642 MPa for recycled concrete aggregates, the values oscillated depending on the test point and date. This high bearing capacity was justified by the excellent material of the subgrade. Nevertheless, the Ev2/Ev1 ratios are lower in this ER with respect to those obtained by Jiménez et al. [10].

In a second work, Jiménez et al. [12] evaluated on an experimental rural road the performance of a recycled aggregate from non-selected CDW. The Ev_2 values was 132 MPa, a lower value than that obtained in this study. The low bearing capacity of the subgrade and the poor quality of the recycled material justified these results.

This new ER has shown that natural materials used are of a high quality possessing a high bearing capacity, and that recycled materials have obtained similar results, which makes them a viable option for NA replacement.

3.3 Deflection results obtained by FWD

In 2009, the road was opened to traffic. From 2009 to 2013, deflection tests were conducted every six months to investigate the evolution of the bearing capacity of these recycled material layers in comparison with NA layers. During this time a total of eight controls were made. FWD represents a more realistic test than loading test plate because it simulates the dynamic load that real traffic generates.

Deflections are shown for subbases (Fig. 11) and bases (Fig. 12) along the investigated road. All deflections are lower than their theoretical values, which means that the structural capacity of the layers is higher than expected.

On subbase layers, deflections and moduli are similar in the three sections, as shown on Fig. 13. On base layers, the mean value of deflections and moduli are close for sections I.I and I.II as shown in Fig. 14. Section I.III has slightly higher deflections and lower moduli values. Table 4 shows the evolution of deflections from June 2009 until January 2013. The deflections obtained are lower than the theoretical values (Fig. 6); this means that the structural capacity of the road is higher than expected. Because the road is coated with an asphalt concrete, and because concrete ditches are located along the road, seasonal variations do not affect the value of the deflections for the three sections.

Three one-way ANOVA tests were performed to determine whether seasonal moisture conditions during deflection measurements had a statistically significant effect on the mean deflections obtained with the FWD for each section. As presented in Table 4, the p-value of the F-test was over 0.05 for the three sections. This means that there was no significant difference in the mean deflections of the sections during wet or dry seasons. Therefore, climate conditions did not affect deflection values. In contrast, as presented in Table 4, there were significant differences in the deflections of the three sections.

Deflection values for section I.II (CS-1+MRS-1) tended to be higher than those for section I.I (CS-1+SS-1). Deflection tended to be minimized in final tests. With respect to section I.III (RMAS-1+MRS-1), the values seem stable, and are higher than those obtained in the two other sections. Values are higher than those obtained by Perez et al. [16] and Agrela et al. [15]. In this Malaga road test, CDW was treated with cement and RC was used for the aggregate, which makes them of better quality than those used in the present research. Deflections showed lower values in section I.I, this was motivated by the higher bearing capacity of SS-1 and CS-1, nevertheless sections build with MRS-1 and RMAS-1 had a suitable performance in the ER. Due to its durability and bearing capacity it can be assure that RMAS-1 and MRS-1 are valid materials for NA substitution as unbound layers.

3.4 Moduli calculations for subbases

Moduli calculations have been made from the deflection basins of the FWD-measured tests from June 2009 to January 2013. To obtain the moduli values, two different methods were used. The first method used back calculation, as described in section 2.6.1 using EVERCAL software [45]. The second method used forward calculation, which is also described in section 2.6.2. GPR and topographic controls were used to determine real thickness of each layer, because moduli obtained through backcalculation are very sensitive to layer thickness.

Moduli for granular subbases SS-1 and MRS-1 are calculated and compared using these two methods. The p-values of both ANOVAs were over 0.05; therefore, there are no significant statistical differences between the mean moduli calculations for each method. Table 5 shows the means and standard deviations for the moduli of SS-1 and MRS-1 using both methods, respectively. It can be concluded that both methods are valid for this calculation. The moduli values obtain in MRS-1 are similar to those back calculated by Lanceri et al. [20] (122−200 MPa). Moduli values obtained are shown on table 5, MRS-1 modulus is between 160.8-156.5 MPa and SS-1 value is between 220.0-223.2 MPa, thus MRS-1 can replace SS-1 with a ratio of 1.4, therefore to obtain the equivalent thickness of a 30 cm layer of SS, 42 cm of MRS-1 are needed. MRS-1 showed an acceptable modulus as a subbase layer in this low bearing traffic road. MRS-1 had a stable mechanical performance during the time that this experiment took place. Therefore, it can be said that it is possible to replace natural soils with MRS on low traffic roads.

3.5 Moduli calculations for bases

The moduli of the granular bases for CS-1 and RMAS-1 are calculated by forward and back calculation, as in the previous section. An ANOVA was performed to evaluate whether or not there was a significant difference between the methods for these two materials. Table 5 presents the means and standard deviations for the moduli of CS-1 and RMAS-1, respectively, using both methods. The ratio of the mean moduli determined from forward-back calculation in CS-1 equals 1.014. For RMAS-1, this ratio equals 1.012, as shown in Table 5 ~~9~~. This implies that both methods are valid for this calculation.

The moduli values obtain in RMAS-1 are similar to those back calculated by Lanceri et al. [20] (235−379 MPa).

Similar results (160−550 MPa) were obtained by Leite et al. [52] for RMA in a laboratory using a repeated load triaxial test. In Table 6, the moduli for granular bases and subbases are reported, according to AASHTO [43]. RMAS-1 would be classified as a natural aggregate because of its modulus, MRS-1 would be classified as a selected soil (S2), SS-1 would be classified as a selected soil (S3), and CS-1 would be classified as a crushed quarry stone.

RA had lower modulus values than NA. Despite this fact, the mechanical performance of RMAS-1 and MRS-1 makes those materials suitable for low volume traffic roads such as the one used in ER.

Moduli results for granular bases are shown on table 5, RMAS-1 modulus is between 351.2-347.0 MPa while CS-1 modulus is between 484.8-477.9 MPa, thus RMAS-1 can replace CS-1 with a ratio of 1.37, therefore to obtain the equivalent thickness of 30 cm of CS-1, 41 cm of RMAS-1 are needed. Moduli of RMAS-1 showed steady values on each FWD test carried out along 5 years, therefore crushed stone can be replaced by RMAS-1 obtaining an acceptable performance. In the same way the MRS-1 can replace the SS-1 with a ratio of 1.40, therefore to obtain the equivalent thickness of 30 cm of SS-1, 42 cm of MRS-1 are needed

3.6 International Roughness Index (IRI)

Two IRI measurements were made on the ER (December 2009 and July 2016). IRI values were obtained as averages of eight passes for each section. In order to detect the effects of the date and the composition of each section on variations in the mean IRI values, a one-way ANOVA was performed. Six different levels were defined, corresponding to the three sections (SI.I, SI.II2 and SI.III) and two measurement dates (2009 and 2016).

The results obtained are presented in Table 7; the results indicate that there were no statistically significant differences between the IRI values for the three sections studied ($p > 0.05$). Likewise, the date has no statistically significant influence on any of the three sections studied ($p > 0.05$). According to the World Bank [41], the values obtained after seven years correspond to a new pavement, and the results are similar for the three sections. There were no significant differences in the behaviour of Section I.I (constructed only with NA) and Section I.III (constructed with CDW aggregates). IRI values obtained after seven years showed the viability of NA substitution by RMAS-1 and MRS-1. This long term period results justifies the use of RMAS-1 and MRS-1 as unbound layers in low volume traffic roads.

4 Conclusions

This research focuses on the mechanical and functional behaviour of an ER built with recycled materials from non-selected construction and demolitions waste mixed with excavation soils (RMAS-1 and MRS-1). The following partial conclusions can be extracted:

RMAS-1 and crushed stone granulometries were very similar. Compaction controls showed that materials were correctly set in place. Dry density was higher and optimum moisture was lower than in natural soils and aggregates; this occurred because of the higher porosity of recycled aggregates.

A high bearing capacity was obtained in sections built with recycled materials, which meet the mechanical requirements of the Spanish regulations for road construction for of any category of traffic. The ratio between E_{v1} and E_{v2} was under 2.2, which is the Spanish limit; this shows that the materials were correctly set in place. Deflections obtained over three years in the experimental road are lower than the theoretical values; this means that the structural capacity of the three sections is higher than expected.

Section I.I built with natural selected soil and crushed limestone exhibited lower deflection values than sections I.II built with mixed recycled soil (MRS-1) and I.III built with mixed recycled soil and recycled mixed aggregates soil (RMAS-1). Section I.II had lower deflection values than Section I.III. Deflections were stable over time and they were under the theoretical limits required for these type of materials.

The determination of moduli through forward and back calculation for the granular bases and subbases showed no statistically significant differences in mean values for the three sections tested. Both methods used were shown to be valid. Because of the simplicity of forward calculation, it is advisable to use that method to determine the moduli of granular bases and subbases for pavements. Crushed limestone had a mean value (between both methods) of 481 MPa, while the value for RMAS-1 averaged 349 MPa. Selected soil had a mean value of 22 MPa, while MRS-1 averaged 158 MPa. Recycled layers had lower moduli values than natural material layers but still had a higher mechanical performance than expected theoretically, thus it can be used as granular bases and subbases in low volume traffic roads. From a practical point of view, 30 cm of selected soil can be replace by 42 cm of MRS-1, and 30 cm of crushed limestone can be replace by 41 cm of RMAS-1.

After seven years during which the ER was open to traffic, IRI performance was shown to be similar in the three sections. According to its value, it could be catalogued by the World Bank as if it was a new pavement. It can be assured that sections built with recycled materials perform similarly to the section made with natural materials, and that its roughness over time is stable.

The long term results obtained by the present work proof the use of RMAS-1 and MRS-1 as viable replacement materials for natural soils and aggregates in low-traffic roads construction (fewer than 50 heavy vehicles/day). Additionally, the technical specification limits for Los Angeles abrasion and sand equivalents in the Spanish code (PG-3) could be raised to 45 for low-traffic roads and mixed recycled aggregates. Finally this research shows new uses for non-selected construction and demolition wastes and prevents its illegal or legal deposit in landfills. Ecological footprint can be reduced by avoiding natural aggregate extraction from rivers and quarries.

I. ACKNOWLEDGMENTS

II. The authors would like to thank the Civil Works Agency of the Regional Government of Andalusia (Agencia de la Obra Pública de la Junta de Andalucía), for its encouragement and support of this research study. We would also like to thank the construction companies Azvi and Geocisa, who made the lab tests, and the pavement survey company GYA.

References

[1] Blengini, G.A., Life cycle of buildings, demolition and recycling potential: A case study in Turin, Italy, Build. Environ. 44 (2009) 319–330. doi:10.1016/j.buildenv.2008.03.007.

[2] Rodríguez, G., C. Medina, F.J. Alegre, E. Asensio, M.I. Sánchez de Rojas, Assessment of Construction and Demolition Waste plant management in Spain: in pursuit of sustainability and eco-efficiency, J. Clean. Prod. 90 (2015) 16–24. doi:10.1016/j.jclepro.2014.11.067.

[3] Eurostat, Waste Stat. Eur. (2014). http://ec.europa.eu/eurostat/ (accessed December 18, 2016).

[4] Mudgal, S., M. Hestin, M. Trarieux, S. Mimid, Contacts BIO Intelligence Service

Véronique Monier Service Contract on Management of Construction and Demolition Waste – SR1 European Commission (DG ENV) In association with, (2011).

[5] Rodríguez-Robles, D., J. García-González, A. Juan-Valdés, J.M. Morán-del Pozo, M.I. Guerra-Romero, Overview regarding construction and demolition waste in Spain, Environ. Technol. 36 (2015) 3060–3070. doi:10.1080/09593330.2014.957247.

[6] European Parliament, Council of the European Union, Directive 2008/56/EC of the European Parliament and of the Council, Off. J. Eur. Union. 164 (2008) 19–40.

[7] Vegas, I., J.A. Ibañez, A. Lisbona, A. Sáez De Cortazar, M. Frías, Pre-normative research on the use of mixed recycled aggregates in unbound road sections, Constr. Build. Mater. 25 (2011) 2674–2682. doi:10.1016/j.conbuildmat.2010.12.018.

[8] García Garrido, M. del L., Estudio de los resultados en obra y a largo plazo de la utilización de materiales reciclados de residuos de construcción y demolición (RCD) en firmes de carreteras y urbanizaciones, (2016). http://hdl.handle.net/11441/40338 (accessed March 29, 2017).

[9] Poon, C.-S., X.C. Qiao, D. Chan, The cause and influence of self-cementing properties of fine recycled concrete aggregates on the properties of unbound sub-base, Waste Manag. 26 (2006) 1166–1172. doi:10.1016/j.wasman.2005.12.013.

[10] Jiménez, J.R., J. Ayuso, F. Agrela, M. López, A.P. Galvín, Utilisation of unbound recycled aggregates from selected CDW in unpaved rural roads, Resour. Conserv. Recycl. 58 (2012) 88–97. doi:10.1016/j.resconrec.2011.10.012.

[11] Jimenez, J.R., F. Agrela, J. Ayuso, M. Lopez, A comparative study of recycled aggregates from concrete and mixed debris as material for unbound road sub-base, 61 (2011) 289–302. http://cat.inist.fr/?aModele=afficheN&cpsidt=24228702.

[12] Jiménez, J.R., J. Ayuso, A.P. Galvín, M. López, F. Agrela, Use of mixed recycled aggregates with a low embodied energy from non-selected CDW in unpaved rural roads, Constr. Build. Mater. 34 (2012) 34–43. doi:10.1016/j.conbuildmat.2012.02.042.

[13] Jiménez, J.R., Recycled aggregates (RAs) for roads, in: Handb. Recycl. Concr. Demolition Waste, 2013: pp. 351–377. doi:10.1533/9780857096906.3.351.

[14] Del Rey, I., J. Ayuso, A. Galvín, J. Jiménez, A. Barbudo, Feasibility of Using Unbound Mixed Recycled Aggregates from CDW over Expansive Clay Subgrade in Unpaved Rural Roads, Materials (Basel). 9 (2016) 931. doi:10.3390/ma9110931.

[15] Agrela, F., A. Barbudo, A. Ramírez, J. Ayuso, M.D. Carvajal, J.R. Jiménez, Construction of road sections using mixed recycled aggregates treated with

cement in Malaga, Spain, Resour. Conserv. Recycl. 58 (2012) 98–106. doi:10.1016/j.resconrec.2011.11.003.

[16] Pérez, P., F. Agrela, R. Herrador, J. Ordoñez, Application of cement-treated recycled materials in the construction of a section of road in Malaga, Spain, Constr. Build. Mater. 44 (2013) 593–599. doi:10.1016/j.conbuildmat.2013.02.034.

[17] Cardoso, R., R.V. Silva, J. de Brito, R. Dhir, Use of recycled aggregates from construction and demolition waste in geotechnical applications: A literature review, Waste Manag. 49 (2016) 131–145. doi:10.1016/j.wasman.2015.12.021.

[18] Jia, X., F. Ye, B. Huang, Utilization of Construction and Demolition Wastes in Low-Volume Roads for Rural Areas in China, Transp. Res. Rec. J. Transp. Res. Board. 2474 (2015) 39–47. doi:10.3141/2474-05.

[19] Park, T., Application of Construction and Building Debris as Base and Subbase Materials in Rigid Pavement, J. Transp. Eng. 129 (2003) 558–563. doi:10.1061/(ASCE)0733-947X(2003)129:5(558).

[20] Lancieri, F., A. Marradi, S. Mannucci, C&D waste for road construction: Long time performance of roads constructed using recycled aggregate for unbound pavement layers, WIT Trans. Ecol. Environ. 92 (2006) 559–569. doi:10.2495/WM060571.

[21] Ullidtz, P., R. Stubstad, Analytical-empirical pavement evaluation using the falling weight deflectometer, (1985). https://trid.trb.org/view.aspx?id=1265522 (accessed December 18, 2016).

[22] AASHTO M145-91, American Association of State Highway and Transportation Officials, Classif. Soils Soil-Aggregate Mix. Highw. Constr. Purp. (2008) 9.

[23] Ministry of Development, Pavement Instruction 6.1 IC: Pavement Sections, Norm. Instr. Construcción. (2003) 41. http://www.fomento.gob.es/NR/rdonlyres/79BE1C89-7C92-425F-9FE4-53A5557CF029/76068/NORMA61IC.pdf.

[24] AENOR, Test for General Properties of Aggregates. Part 1: Methods for Sampling; UNE-EN 932-1:1997, Asociacion Española de Normalizacion, 1997.

[25] AENOR, Tests for general properties of aggregates Ð Part 2 : Methods for reducing laboratory; UNE-EN 932-2:1999, Asociacion Española de Normalizacion, 1999.

[26] AENOR, Tests for Geometrical Properties of Aggregates—Part 11: Classification Test for the Constituents of Coarse Recycled Aggregate; UNE-EN 933-11:2009, Asociacion Española de Normalizacion, 2009.

[27] Agrela, F., M. Sánchez De Juan, J. Ayuso, V.L. Geraldes, J.R. Jiménez, Limiting properties in the characterisation of mixed recycled aggregates for use in the manufacture of concrete, Constr. Build. Mater. 25 (2011) 3950–3955. doi:10.1016/j.conbuildmat.2011.04.027.

[28] Ministry of Development, General technical specifications for road works and bridges (PG-3), Ministerio de Fomento, Centro de Publicaciones, 2004.

[29] Public Works Agency of the Regional Government of Andalusia, Catalogue of pavements and work units with RA from CDW., 2016. http://www.aridosrcdandalucia.es/rcd/wp-content/uploads/2017/03/Libro-catalogo-de-firmes-vers-impresa-en-pdf.pdf (accessed August 25, 2017).

[30] AENOR, Tests for Geometrical Properties of Aggregates—Part 1: Determination of Particle Size Distribution—Sieving Method; UNE-EN 933–1, Asociacion Española de Normalizacion, 2012.

[31] ASTM D6938 - 15 Standard Test Methods for In-Place Density and Water Content of Soil and Soil-Aggregate by Nuclear Methods (Shallow Depth), (n.d.). https://www.astm.org/Standards/D6938.htm (accessed December 18, 2016).

[32] AENOR, Load test of plate soils; UNE 103808:2006, Asociacion Española de Normalizacion, 2006.

[33] Ministry of Development, Pavement Rehabilitation Instruction 6.3IC, Ministerio de Fomento, Centro de Publicaciones, 2003.

[34] Public Works Agency of the Regional Government of Andalusia, PPTG ADAR. General technical specifications for high-performance dynamic monitoring tests, 2004. http://www.aopandalucia.es/inetfiles/area_tecnica/Calidad/ADAR/pliego_prescripciones_ADAR.pdf (accessed November 18, 2017).

[35] Korswagen, A.R., D.. De Jong, M.G.. Peutz, Computer program BISAR : layered systems under normal and tangential surface loads (external report), Shell Research, 1973. http://library.brrc.be/opac_css/index.php?lvl=notice_display&id=44410 (accessed December 18, 2016).

[36] Burmister, D.M., The General Theory of Stresses and Displacements in Layered Systems. I, J. Appl. Phys. 16 (1945) 89. doi:10.1063/1.1707558.

[37] Acum, W.E.A., L. Fox, Computation of Load Stresses in a Three-Layer Elastic System, Géotechnique. 2 (1951) 293–300. doi:10.1680/geot.1951.2.4.293.

[38] Schifmann, R.L., General Analysis of stresses and displacements in layered elastic systems, 203 (1962).

[39] Public Works Agency of the Regional Government of Andalusia, Pavement instruccion of Andalusia, (2007). http://www.juntadeandalucia.es/fomentoyvivienda/portal-web/web/publicaciones/3707 (accessed December 18, 2016).

[40] Huang, Y.H., Pavement analysis and design, Prentice Hall, 1993.

[41] Sayers, M.W., T.D. Gillespie, W.D.O. Paterson, Guidelines for conducting and calibrating road roughness measurements, World Bank, 1986.

[42] ASTM E867 - 06(2012) Standard Terminology Relating to Vehicle-Pavement Systems, (n.d.). https://www.astm.org/Standards/E867.htm (accessed December 18, 2016).

[43] American Association of State Highway and Transportation Officials., National Cooperative Highway Research Program., AASHTO guide for design of pavement structures., AASHTO, 1988.

[44] Tayabji, S.D., E.O. Lukanen, Nondestructive testing of pavements and backcalculation of moduli : Third volume, ASTM, 2000.

[45] Washington State Department of Transportation, Everseries Users Guide, (2005).

[46] Cauwelaert, V.F., Pavement Design and Evaluation : The required Mathematics and Applications, 2004.

[47] Stubstad, R.N., Y.J. Jiang, E.O. Lukanen, Guidelines for Review and Evaluation of Backcalculation Results, (2006).

[48] Hogg, A.H.A., XXXIII. Equilibrium of a thin slab on an elastic foundation of finite depth, London, Edinburgh, Dublin Philos. Mag. J. Sci. 35 (1944) 265–276. doi:10.1080/14786444408520878.

[49] Wiseman, G., J. Uzan, M.S. Hoffman, I. Ishai, M. Livneh, Simple elastic models for pavement evaluation using measured surface deflection bowls, in: Fourth Int. Conf. Struct. Des. Asph. Pavements, Ann Arbor, Mich., 1977. http://ent.library.utm.my/client/en_AU/main/search/detailnonmodal/ent:$002f$002fSD_ILS$002f268$002fSD_ILS:268593/ada;jsessionid=3A9F42E996C1E5D431D93F990722160B?qu=Pavements+--+Testing&ic=true&ps=300 (accessed December 18, 2016).

[50] Dorman, G.M., Metcalf, Design curves for flexible pavements based on layered system theory, Highw. Res. Rec. (1965).

[51] Brown, S.F., Soil mechanics in pavement engineering, Géotechnique. 46 (1996) 383–426. doi:10.1680/geot.1996.46.3.383.

[52] Leite, F.D.C., R.D.S. Motta, K.L. Vasconcelos, L. Bernucci, Laboratory evaluation of recycled construction and demolition waste for pavements, Constr. Build. Mater. 25 (2011) 2972–2979. doi:10.1016/j.conbuildmat.2010.11.105.

TABLE CAPTIONS

Table 1. Composition of the mixed recycled aggregate. UNE-EN-933-11:2009.

Table 2. Physico-mechanical and chemical properties of unbound materials.

Table 3. Hogg model coefficients.

Table 4. Deflection results of ANOVA.

Table 5. Moduli of SS-1, MRS-1, CS-1 and RMAS-1 (MPa). Summary of comparison between forward and backcalculation.

Table 6. Maximum values for granular bases and subbases according to ICAFIR [38].

Table 7. International Roughness Index results of ANOVA.

FIGURE CAPTIONS

Fig. 1. Experimental Road cross sections.

Fig. 2. Flow diagram in the recycling plant.

Fig. 3. Particle size distribution curves of ER granular bases.

Fig. 4 Average monthly maximum and minimum temperatures.

Fig. 5 Monthly total precipitation (mm).

Fig. 6 Layer mechanical properties for the three sections (adapted from García-Garrido [8]).

Fig. 7 Densities and moistures in subbases.

Fig. 8 Densities and moistures in bases.

Fig. 9 Plate tests results on granular subbases.

Fig. 10 Plate tests results on bases.

Fig. 11 Bearing capacity of granular subbase (12th May 2009). Adapted from García-Garrido [8].

Fig. 12 Bearing capacity of granular base (19th and 21th 2009). Adapted from García-Garrido [8].

Fig. 13-Deflections over granular subbase (May, 2009).

Fig. 14 Deflections over granular base course (May, 2009).

Table 1. Composition of the mixed recycled aggregate. UNE-EN-933-11:2009.

		MRS-1	RMAS-1
Class	Type	Weight	Weight
R_A	Asphalt	0	0
R_B	Ceramics	5.3	2.5
R_C	Concrete and Mortar [a]	16.5	42.56
R_L	Lightweight particles	0	0
R_U	Unbound aggregates [b]	1.9	40.57
X_1	Natural Soil [c]	75.4	13.57
X_2	Others [d]	0.9	0.8
	Total	100	100

[a] Natural aggregates with cement mortar attached from concrete or masonry

[b] Natural aggregates without cement mortar attached

[c] Excavation soil.

[d] Wood, glass, plastic, metals, gypsum.

Table 2. Physico-mechanical and chemical properties of unbound materials.

		Materials					Standard
Properties		SG-1	SS-1	MRS-1	RMAS-1	CS-1	
Grading	Max. Size (mm)	12.5	80	25	20	25	UNE 103101:1995
	% passing sieve # 0.063	39.9	14.3	18	13	13.8	UNE 103101:1995
Atterberg Limits	Liquid Limit	23.8	-	24.6	23.4	-	UNE 103103:1994 UNE 103104:1993
	Plastic Limit	11.2	-	17.8	18.6	-	UNE 103103:1994 UNE 103104:1993
	Plastic Index	12.6	-	6.8	4.6	-	UNE 103103:1994 UNE 103104:1993
	Sand equivalent (%)				27.4	42.2	UNE-EN 933-8:2000
	Los Angeles (%)				42	28	UNE-EN 1097-2:2010
	Flakiness index (%)				23	8	UNE-EN 933-3:2012
	Crushed particles (%)				100	100	UNE-EN 933-35:1999
Modified Proctor	Max. Density (Mg/m^3)	1.6	2.1	1.8	1.94	2.38	UNE 103501:1994
	Optimum Moisture (%)	10	9	14.5	10.5	7	UNE 103501:1994
C.B.R.(*)	100%	5.9	74.4	56	65.5	100.7	UNE 103502:1995
	95%	3	42.3	38.9	35.3	66.6	UNE 103502:1995
	Swelling after 4 days soaking (%)		0.2	0.1	0.1	0	UNE 103502:1995
	Acid-soluble sulphate (%SO_3)		0.13	0.92	0.31		UNE 103201:2003
	Organic matter (%)	2.51	0.11	1.04	0.92		UNE 103204:1993

(*) The CBR tests were carried out with laboratory samples compacted at their corresponding maximum dry density of Modified Proctor and 4-day of soaked conditions

Table 3. Hogg model coefficients.

CASES		I	II	III
Depth to hard bottom	h/l_0	10	10	Infinite
Poisson´s ratio	μ_0	0.50	0.40	All values
Influence factor	I	0.1614	0.1689	0.1925
Range Δ_r/Δ_0		> 0.70	> 0.426	All values
$r_{50}=f(\Delta_r/\Delta_0)$	α	0.592	0.548	0.584
	β	2.460	2.629	3.115
	B	0	0	0
Range Δ_r/Δ_0		< 0.70	< 0.426	
$r_{50}=f(\Delta_r/\Delta_0)$	α	0.219	0.2004	
	β	371.1	2283.4	
	B	2	3	
$l=f\ (r_{50}, \alpha)$	y_0	0.620	0.602	0.525
	m	0.183	0.192	0.180
$S_0/S = f\ (a/l)$	$\overline{m}$	0.52	0.48	0.44

Table 4. Deflection results of ANOVA.

		Factor									
		Composition of Sections			Date						
Properties	Factor Levels	Section I.I	Section I.II	Section I.III		Section I.I		Section I.II		Section I.III	
Deflections (0.01 mm)	p-value		<0.0001			0.7115		0.2529		0.8125	
	M	45.98	58.06	70.50	Factor Levels	M	SD	M	SD	M	SD
	SD	6.41	11.63	14.60	jun-09	49.11	8.05	64.34	5.95	66.81	9.55
					dic-09	44.49	7.41	59.42	8.47	67.40	21.50
					jun-10	46.99	8.67	57.10	14.98	65.54	12.84
					dic-10	46.15	7.18	61.77	12.50	74.99	18.21
					jul-11	46.20	6.04	62.03	12.36	71.32	16.44
					dic-11	45.98	6.90	55.86	16.37	75.16	16.05
					jun-12	46.25	3.20	51.20	8.25	69.02	12.42
					ene-13	42.63	1.60	52.74	8.19	73.78	8.41

M=Mean

SD=Standard deviation

Table 5. Moduli of SS-1, MRS-1, CS-1 and RMAS-1 (MPa). Summary of comparison between forward and backcalculation.

Method	SS-1		MRS-1		CS-1		RMAS-1	
	M	SD	M	SD	M	SD	M	SD
Back moduli	223.2	21.3	160.8	29.4	484.8	96.4	351.2	57.1
Forward moduli	220.0	32.7	156.5	31.3	477.9	97.9	347.0	68.9
p-value	0.5136		0.2613		0.5671		0.7073	

M (Mean), SD (Standard Deviation).

Table 6. Maximum values for granular bases and subbases according to ICAFIR [38]**.**

Material	Maximum Moduli (MPa)
A-4 (AASHTO)	150
A-3 (AASHTO)	200
A-1-b (AASHTO)	250
A-1-a (AASHTO)	350

Table 7. International Roughness Index results of ANOVA.

Properties	Factor Levels	Composition of Sections: Section I	Composition of Sections: Section II	Composition of Sections: Section III	Date: Factor Levels	Date: Section I M	Date: Section I SD	Date: Section II M	Date: Section II SD	Date: Section III M	Date: Section III SD
IRI (mm/m)	p-value		0.3405			0.4947		0.7138		0.1913	
	M	2.28	2.60	2.48							
	SD	0.80	0.52	0.59	dic-09	2.17	0.90	2.56	0.65	2.33	0.67
					jul-16	2.38	0.70	2.64	0.36	2.63	0.48

M=Mean

SD=Standard deviation

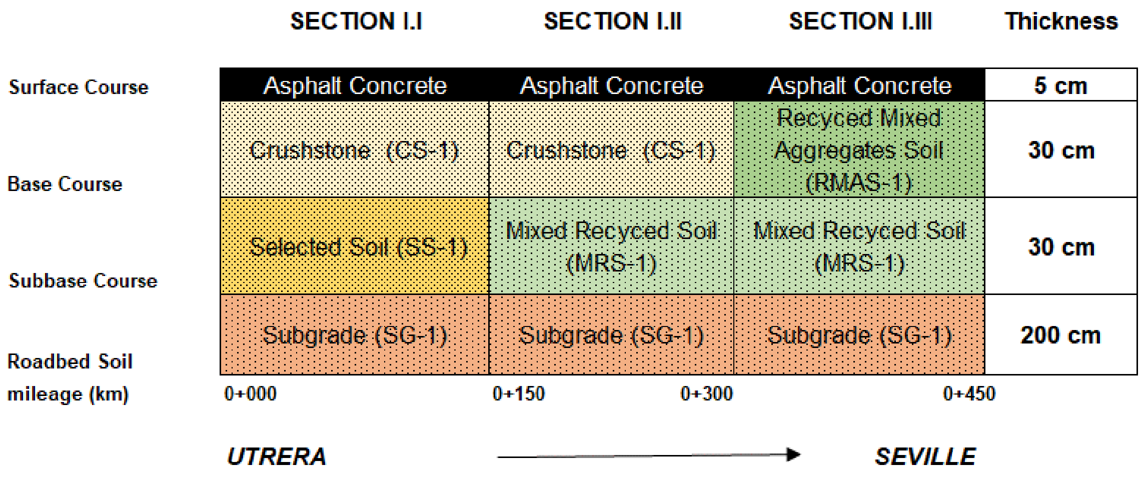

Fig. 1. Experimental Road cross sections.

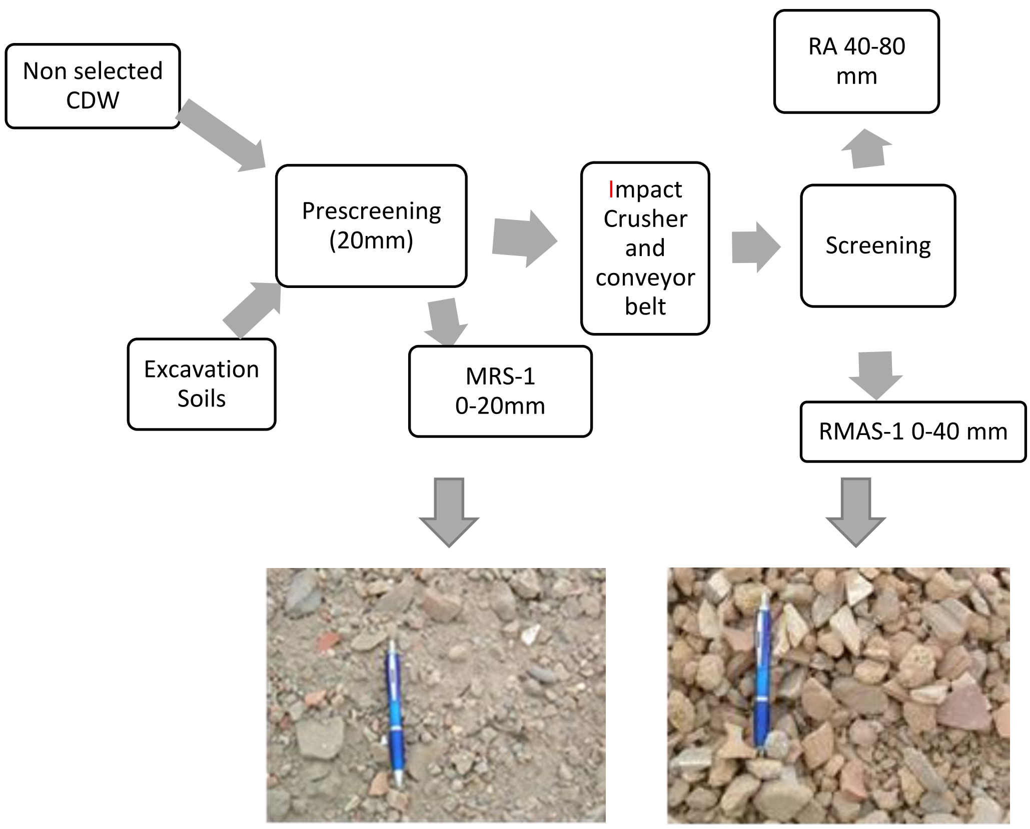

Fig. 2. Flow diagram in the recycling plant.

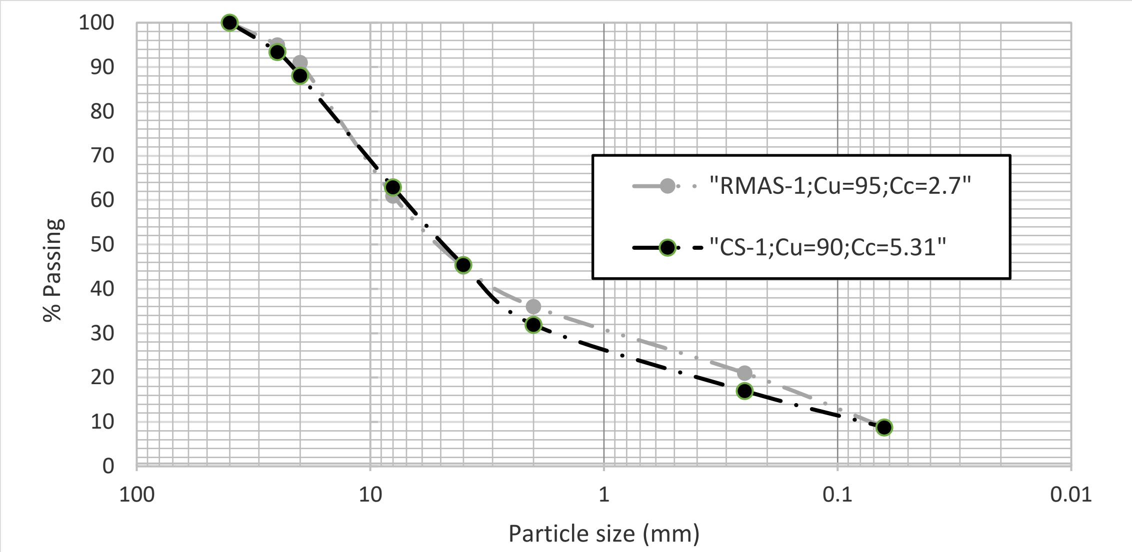

Fig. 3. Particle size distribution curves of ER granular bases.

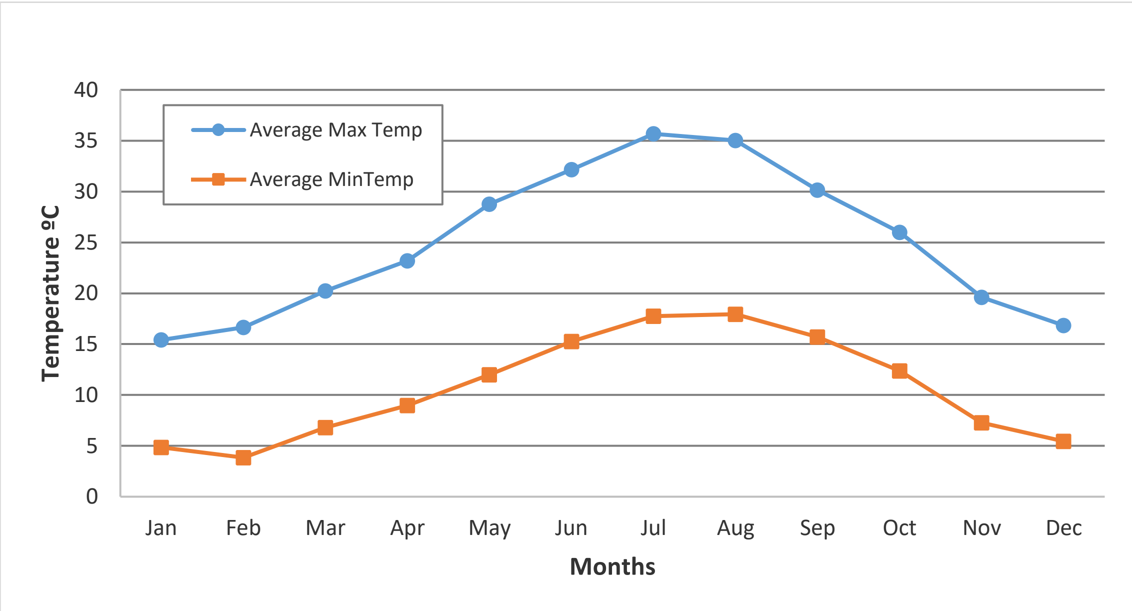

Fig. 4. Average monthly maximum and minimum temperatures.

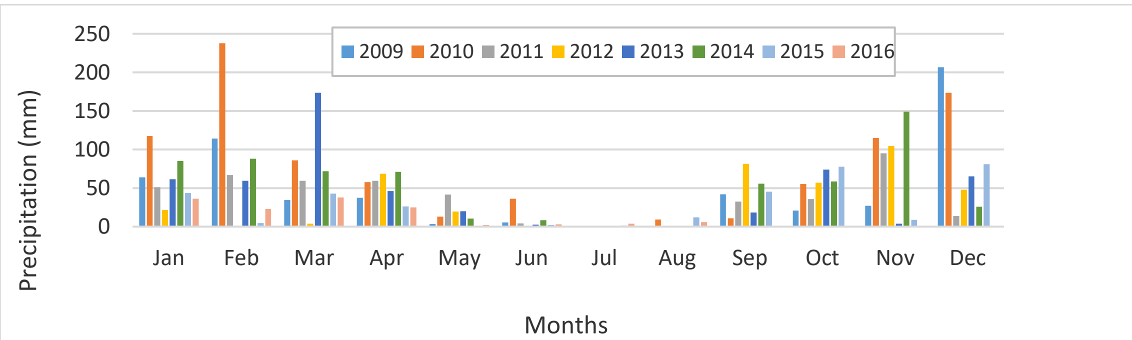

Fig. 5. Monthly total precipitation (mm).

	Layer	Thichness		Modulus (MPa)	Poisson´s ratio	Theoretical deflection mm/100
	Base Course	5 cm	E1	**6000**	**0,33**	**149**
	Granular Base	30 cm	E2	**225**	**0,35**	**241**
	Subbase	30 cm	E3	**75**	**0,35**	**238**
	Roadbed Soil CBR=3	200 cm	E4	**30**	**0,35**	**-**

Fig. 6. Layer mechanical properties for the three sections (adapted from García-Garrido [8]).

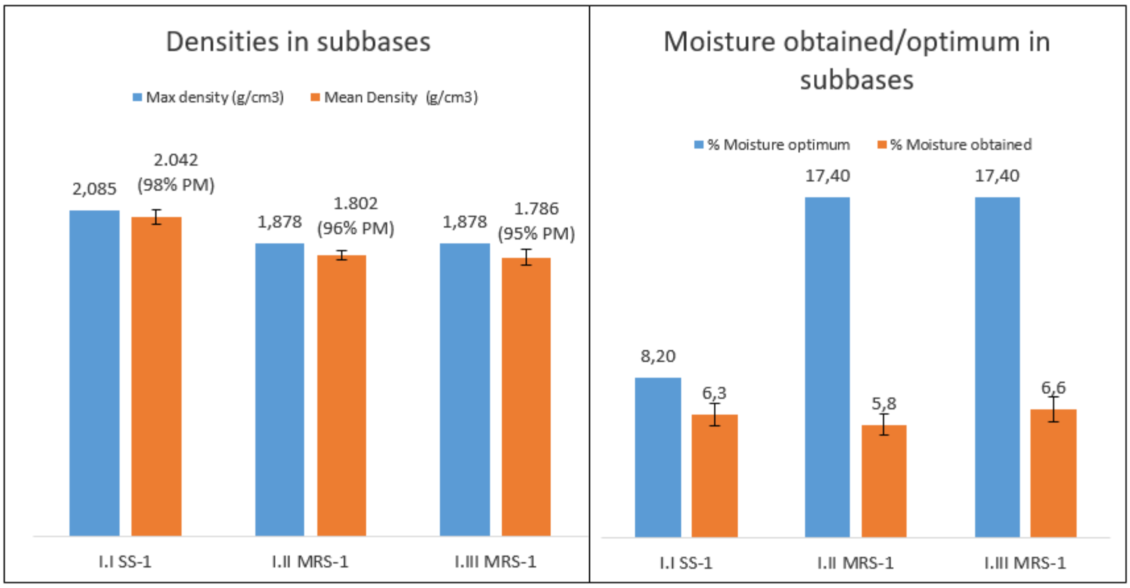

Fig. 7. Densities and moistures in subbases.

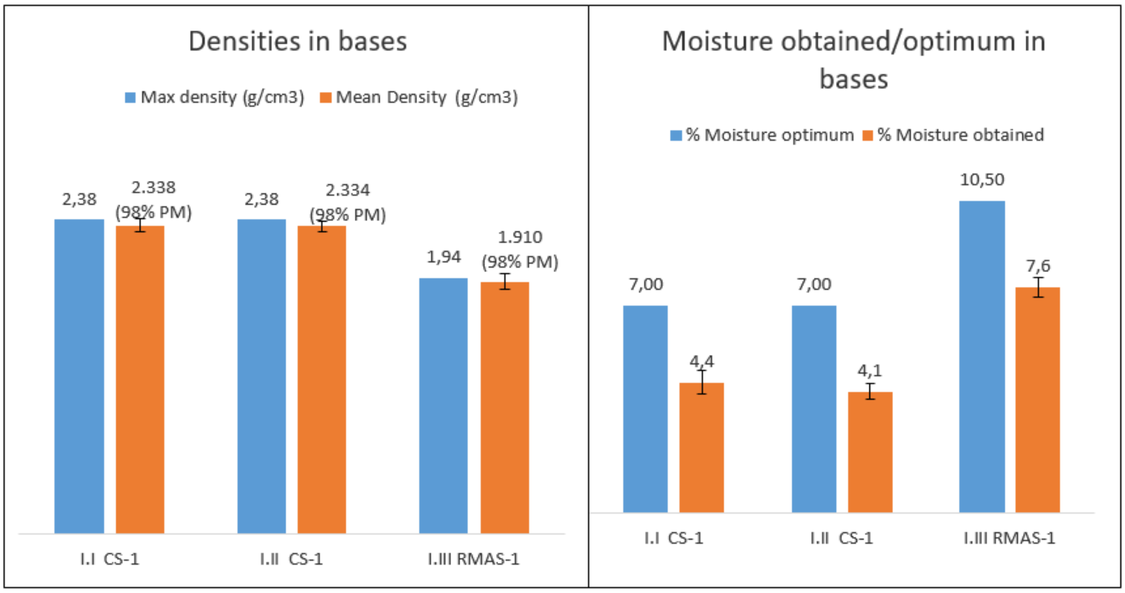

Fig. 8. Densities and moistures in bases.

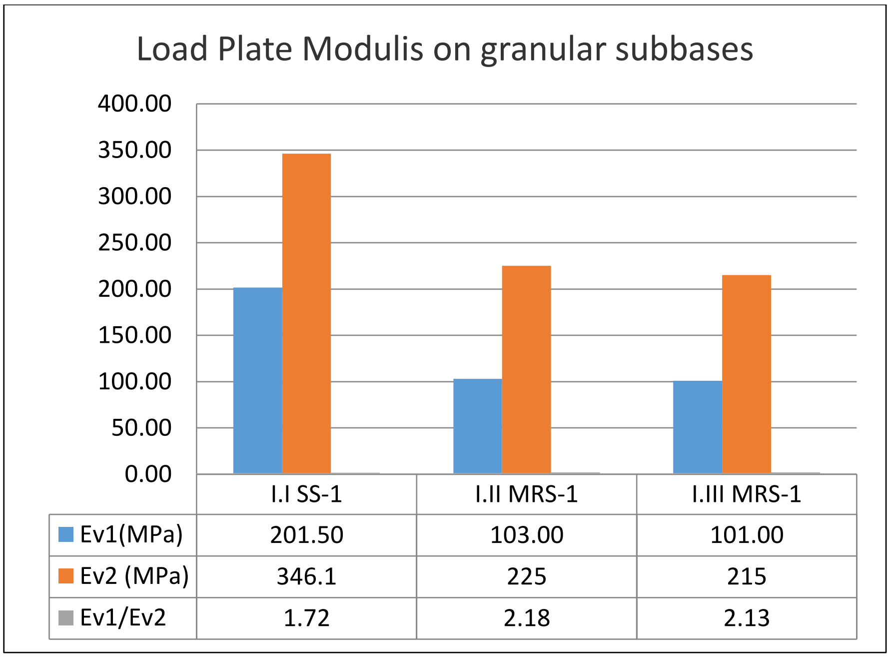

Fig. 9. Plate tests results on granular subbases.

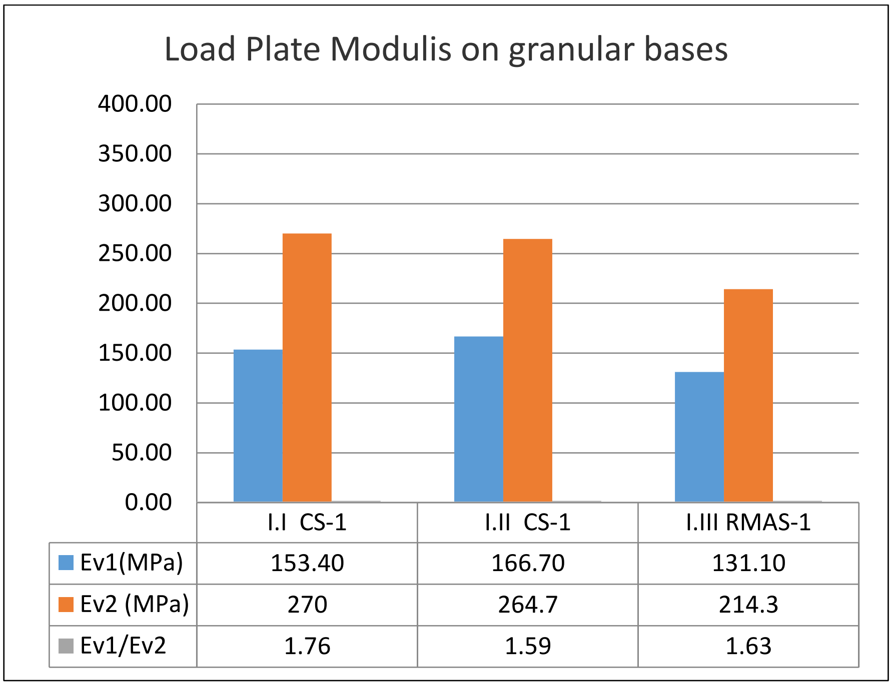

Fig. 10. Plate tests results on bases.

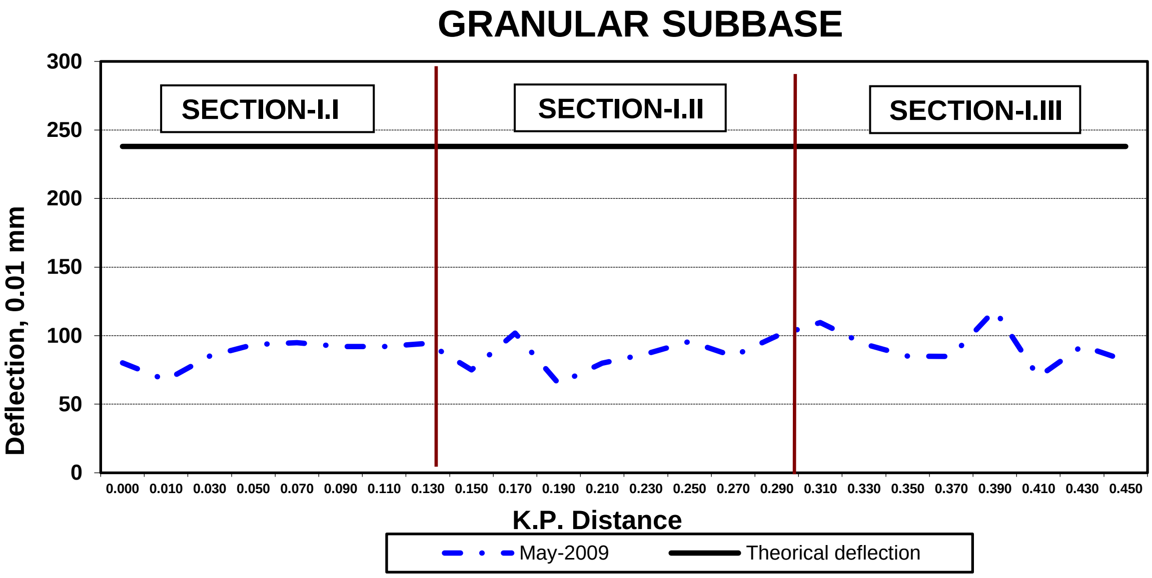

Fig. 11. Bearing capacity in granular subbase (12th May 2009). Adapted from García-Garrido [8].

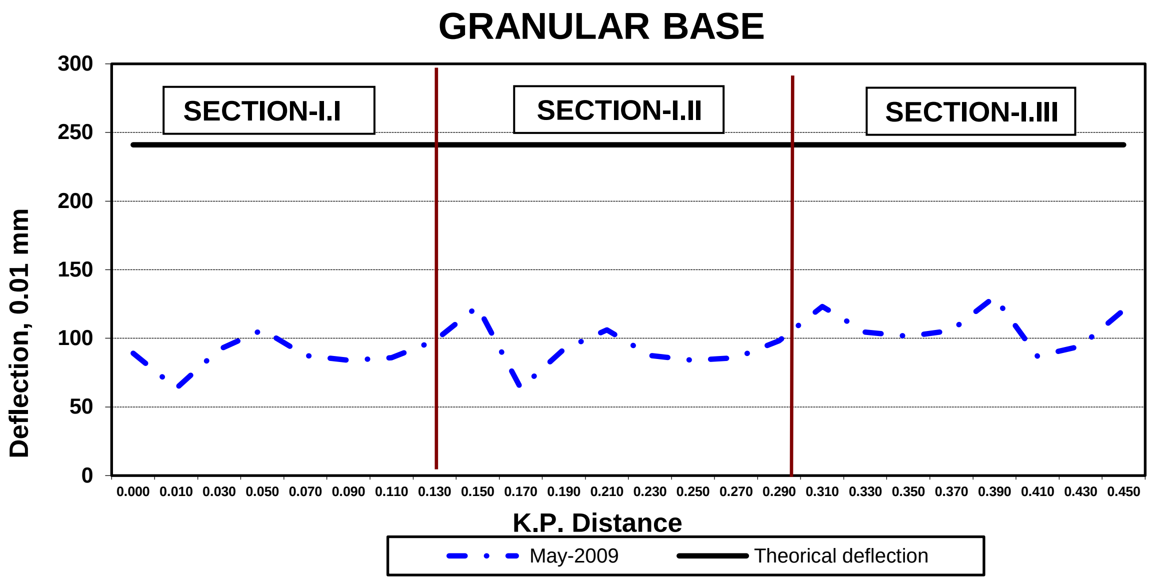

Fig. 12. Bearing capacity in granular base (19th and 21th May 2009). Adapted from García-Garrido [8].

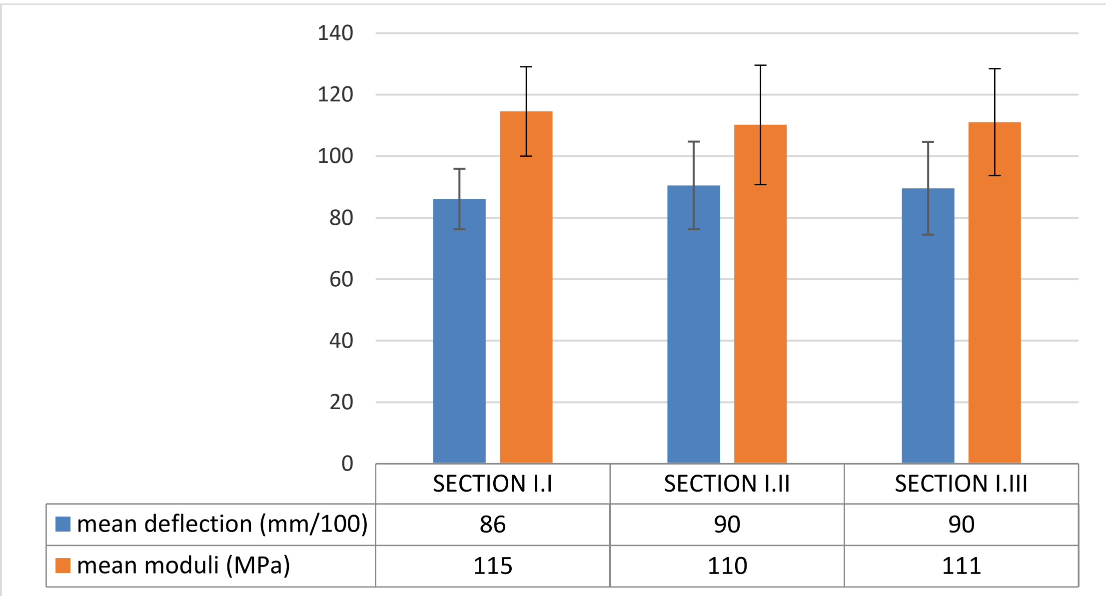

Fig. 13. Deflections over granular subbase (May, 2009).

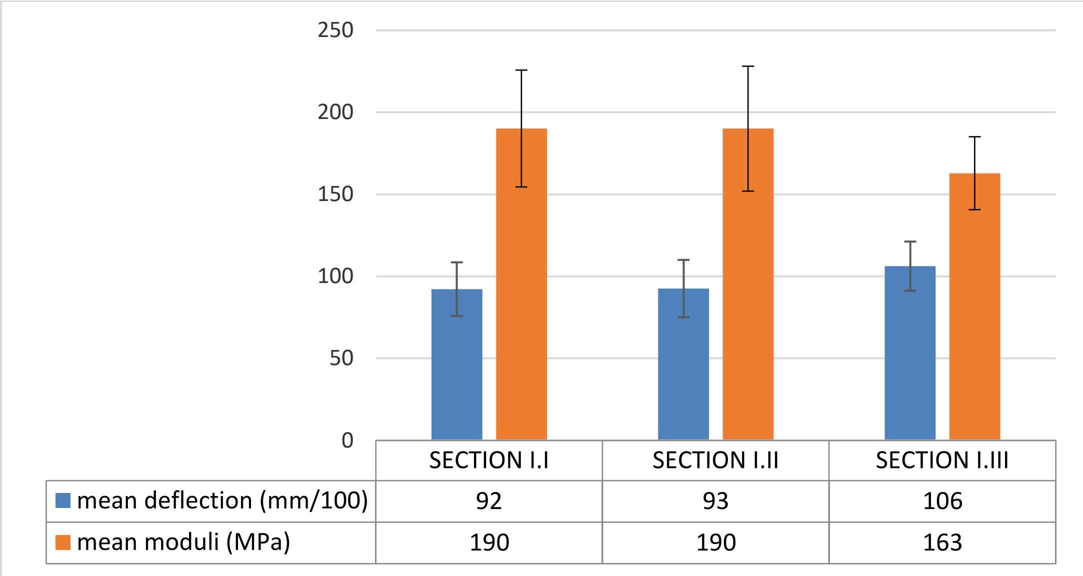

Fig. 14. Deflections over granular base course (May, 2009).